Functional Materials 12, No.4 (2005)

Doped sillenite crystals

T.V.Panchenko, N.A.Truseeva*, K.Yu.Strelets*

Dnepropetrovsk National University, 49050, Dniepropetrovsk, Ukraine
*Dneprodzerzhinsk State Technical University,
51918 Dneprodzerzhinsk, Ukraine

Al, Ga, Cr, Mn, V, Cu, Mo, Fe, Sn doped $Bi_{12}SiO_{20}$ crystals and pure $Bi_{12}SiO_{20}$ crystals with varying concentration of non-stoichiometric defects have been grown. The localization of the doping ions in the crystal lattice have been determined and the distribution coefficients thereof have been calculated within the frame of isomorphism theory considering the energy of preference to the octahedron oxygen surrounding. The means to improve the optical quality of the pure and doped $Bi_{12}SiO_{20}$ crystals have been proposed, the photochromic properties thereof have been investigated.

Выращены кристаллы $Bi_{12}SiO_{20}$ с варьируемой концентрацией дефектов нестехиометрии и легированные ионами Al, Ga, Cr, Mn, V, Cu, Mo, Fe, Ag и Sn. В рамках теории изоморфизма с учетом энергии предпочтения к октаэдрическому кислородному окружению определена локализация примесных ионов в кристаллической решетке, найдены коэффициенты их распределения. Предложены способы повышения оптического качества чистых и легированных кристаллов $Bi_{12}SiO_{20}$, исследованы их фотохромные свойства.

The sillenite crystals $Bi_{12}MO_{20}$ (BMO, with M=Si, Ge, Ti) are known as photorefractive materials of a high photosensitivity (~10^{-6} J·cm^{-2}). Those work successfully as functional media in different types of light-modulating and other devices of solid-state electronics and in holographic systems of optical information record and storage. The search for the ways to modification of BMO properties and optical quality improvement seems to be very urgent.

A series of doped sillenites have been grown to date [1–4]. It has been shown that the doping influences essentially their electrical and optical properties. However, to understand the role of the doping ions and intrinsic defects, it is necessary to determine the charge state and local symmetry thereof in BMO crystals. It is important to improve the optical quality by optimizing the growth conditions of intentionally undoped and doped BMO crystals. This work presents the investigation results of these problems for $Bi_{12}SiO_{20}$ (BSO).

The BSO crystals were grown by Czochralski method. The dopants were introduced to the charge according to the stoichiometric (1, 2) and super stoichiometric (3) relations:

$$6(1-x)Bi_2O_3 + 6\cdot xMe_2O_3 + SiO_2 = Bi_{12(1-x)}Me_{12\cdot x}SiO_{20}, \quad (1)$$

$$6Bi_2O_3 + xMeO_2 + (1-x)SiO_2 = Bi_{12}Me_{Si_{1-x}}O_{20}, \quad (2)$$

$$6Bi_2O_3 + xMe_nO_m + SiO_2 = Bi_{12}Me_xSiO_{20}, \quad (3)$$

where $0.04 \geq x \geq 0.0004$; Me = Al, Ga, Cr, Fe, V, Cu, Ag, Mn, Mo, Sn as oxides: Me_2O_3 (Al_2O_3, Ga_2O_3, Cr_2O_3, Fe_2O_3), MeO_2 (MnO_2, MoO_2, SnO_2) and Me_nO_m (CuO, V_2O_5, Ag_2O, where $n = 1; 2$; $m = 1$ to 5). Concentration of impurities have been determined by the spectral emission analysis using a PGS-2 diffraction spectrograph, the variation coefficient not exceeding 6.07 %. The crystal quality was estimated basing on the presence of blocks and phases inclusions (differential thermal (DTA) and X-ray analysis),

contents of defects and dislocations (by microscopy), the uncontrolled impurity concentration (spectral emission analysis), the presence of mechanical stresses (optical polarization method), the presence of optically and photoelectrically active defects (optical absorption spectroscopy and photoconductivity). The spectra of optical absorption ($\alpha_0(h\nu)$, $\alpha^{ph}(h\nu)$) and photoconductivity ($\sigma_0{}^{ph}(h\nu)$, $\sigma_i{}^{ph}(h\nu)$) prior to ($\alpha_0(\nu)$, $\alpha_0{}^{ph}(\nu)$) and after ultraviolet or blue-green exposure ($\alpha^{ph}(h\nu)$, $\sigma_i{}^{ph}(h\nu)$ corresponding to the stationary (prior to the exposure) and excited (after the exposure) states of BSO were investigated in the $h\nu = 0.4$ to 3.4 eV range. The absorption change spectra $\Delta\alpha^{ph}(h\nu) = \alpha^{ph}(h\nu) - \alpha_0(h\nu)$ characterizing the photochromic effect (PCE) were analyzed, too. The optical transmission spectra $t(\lambda)$ were measured by Cary-5E, Specord M40, Specord NIR61 spectrophotometers. The measurements were carried out using polished plane-parallel plates of 0.03 to 5 mm thickness and with large (001) surfaces. The absorption spectra were calculated using the known relation:

$t = \{(1 - R^2)\times[1 + \alpha\lambda(4\pi n)^{-2}]\}/\{\exp(-\alpha d) - R^2\exp(-2\alpha d)\}$, where $R(\lambda) = [(n - 1)/(n + 1)]^2$ are the reflection spectra. The refraction dispersion was determined in the $\lambda = 0.4$ to 0.7 μm range on the prisms using a GS-5 goniometer and a MDR-12 monochromator. For the $\lambda' = 0.3$ to 0.4 and $\lambda'' = 0.7$ to 3 μm ranges, $n(\lambda)$ were calculated using the known relation: $n^2(\lambda) = A + B\lambda^2/(\lambda^2 - \lambda_{01}{}^2) + C\lambda^2/(\lambda^2 - \lambda_{02}{}^2)$, where $A = 92.22$ μm^{-2}, $B = 0.534$ μm^{-2}, $\lambda_0 = 0.22$ μm. The photoconductivity spectra in the $h\nu = 0.5$ to 3.3 eV range have been measured in a constant electrical field using a SPM-2 monochromator and the synchronic detection technique on the planar samples cut out in the (001) plane. A 600 W xenon lamp was used as the light source. The silver electrodes were applied by vacuum burning-in. The measurements were carried out at $T_1 = 200$ to 300 and $T_2 = 80$ to 90 K. The PCE was excited by a 400 W mercury lamp in the $h\nu = 2$ to 3.3 eV range. The state of samples after heating to 800 K and subsequent slow cooling (for 24 hours) to T_1 or T_2 temperature was considered to be the stationary one.

Undoped and doped BSO crystals were grown by the Czochralski method. The empirically selected temperature regimes were provided by the temperature control system to within ~0.1 K. The crystallization probability of metastable phases was lowered due to axial symmetry of the heat field and the lowered temperature gradient in the melt down to 10 K/cm. Platinum crucibles of 350 cm^3 volume were used. Platinum dissolution in the BSO melt was observed. However, the spectral emission analysis has shown that essentially no platinum was present in the BSO crystals (less that 0.001 mass. %) if the charge has not been used completely (less than 70 %). The optimum crystal pulling rate ν and the seed rotation speed w were as follows: $\nu = 1.6$ to 4.8 mm/h, $w = 40$ to 60 rpm. The further ν increase results in deterioration of the crystal quality due to increasing number of dislocations, which is connected with the rebuilding of the short-range structure of the melt into the sillenite structure. If the transition has sufficient time to occur in the precrystalline layer (in this case, at $\nu <$ mm/h), the dislocation density decreases.

The seed rotation speed influences the surface morphology of the BSO crystal. As w increases from 0 to 60 rpm, the crystallization front shape changes from convex (towards the melt) to flat or concave. For the convex front, $(\partial T/\partial h)/(\partial T/\partial r) = h/r$, where $\partial T/\partial h$, $\partial T/\partial r$ are the axial and radial temperature gradients, respectively; h and r, the height of the crystallization spherical surface and the crystal radius, respectively. The axial temperature gradient is not influenced by the melt mixing, but $\partial T/\partial r$ decreases with the increasing w and crystallization front becomes plane. The crystal diameter stability depends upon w, too.

The BSO single crystal structure depends on the accuracy of the seed crystallographic orientation. Therefore, the BSO crystals have been oriented in the direction [100], [110] or [111] to within 5–8′ using an X-ray diffractometer. The most perfect BSO crystals with a low dislocation density ($N_{ds} < 10^2$ cm^{-2}) have been grown in the [100] direction. At other growth directions, the dislocation density increases, e.g. $N_{ds} \sim 10^3$ and ~10^5 cm^{-2} at growing in the [111] and [100] directions. When w is less than 20 rpm, the crystal cross section is almost circular. At 40–60 rpm, the crystallization front is flat at the [001] growth direction. The pulling speed ν in its optimum limits does not influence the dislocation density. The homogeneity region of sillenite phase in Bi_2O_3–

Table 1. Non-stoichiometry influence on BSO crystal properties and homogeneity

Parameter γ, Characteristics	10	10.5	10.9	11.5	13.5
σ_0^{ph}, $\Omega \cdot cm^{-1}$ ($h\nu$ = 2.6–2.4 eV)	10^{-10}	$2 \cdot 10^{-10}$	$2.8 \cdot 10^{-10}$	$3.1 \cdot 10^{-10}$	$1.3 \cdot 10^{-10}$
α_0, cm^{-1} ($h\nu$ = 2.8–2.0 eV)	137–49	127–40	117–33	151–41	265–118
Microscopic heterogeneity	##;)) ; ❒	##	••	••	••
Light transmission in crossed polaroids, t, a.u.	40–50	30–50	25–30	25–30	40–50
$\Delta\alpha^{ph}$, cm–1 ($h\nu$ = 2.6–2.4 eV)	7–10	5–8	5–8	10–12	15–20

Notes:)) — fine cracks; ❒ — blocks; ##, #— coarse inclusions of about 10^{-2} cm size in the crystal bulk; •• — inclusions of about 10^{-3} cm size in crystal bulk and separate.

SiO_2 system is 13.2–5.7 mol %. SiO_2 [5]. The stoichiometric mixture consists of 14.3 % mol. of SiO_2 and 85.7 mol %. of Bi_2O_3. The crystal is not homogeneous along the crystal growing axis in the homogeneous region of the charge. This heterogeneity is caused by the difference between the evaporation rates of Bi_2O_3 and SiO_2 from the melt, the replacement of Si ions by Bi ions with the formation of γ-phase Bi_2O_3 ($Bi_{24}Bi_3 + Bi_5 + O_{40}$) which is isomorphic and isostructural to the BSO phase, and the adsorption of CO_2 with $Bi_2O_3 \cdot CO_2$ formation. We have investigated the influence of the charge composition variation γ from stoichiometry (γ = 12) ranging in $10 < \gamma < 13.5$ upon the $Bi_\gamma SiO_{1.5\gamma+2}$ crystal quality. The optical homogeneity, the photoconductivity and the optical absorption in the blue-green spectral region (where the optical information is recorded on sillenite crystals) and PCE were the quality criteria. The optimum is γ = 10.9–11.5 (Table 1).

To obtain high quality crystals, a specific method of the charge preparation is to be used. It comprises the Bi_2O_3 and SiO_2 powders dispersion to the grain size of 1–5 μm, homogenization of their mixture with alcohol by grinding and mixing in an agate mill, pressing of the homogeneous mixture into tablets and sintering of the tablets. The DTA of the charge and the optical control of microscopic heterogeneities in the crystals has shown that a considerable improvement of BSO crystal optical quality is provided by the following conditions: the charge grinding time 3.5 to 4 h; synthesis temperature 1020 K; synthesis duration 10 to 20 h. The purification procedure by crystallization is as follows. After the 1st crystallization, the BSO crystals (γ = 10.9–12) were used to prepare a melt and the 2nd crystallization was effected. Similarly, melts of BSO crystals obtained after the 2nd and 3rd crystallizations were used in the 3rd and the 4th crystallizations. We have found that the best purification of the crystal from the uncontrolled impurity is achieved, being accompanied by enrichment of the slag which remains in the crucible. The 2nd crystallization provides the optimum combination of the optical homogeneity, high photoconductivity, low optical absorption, and PCE in the blue-green region of the spectra (Table 2).

Regular striate microheterogeneity in longitudinal section similar to that studied before in $Pb_5Ge_3O_{11}$ is a typical optical heterogeneity of BSO crystals. But unlike $Pb_5Ge_3O_{11}$, it appears in BSO crystals only after annealing in air (for 48 h at $T_a \approx 900$ K) or in nitrogen (for 10–15 h at $T_a \approx 770$ K). It is weakened in the crystals annealed in oxygen or in air at $T_a \leq 800$ K. The monotonous heterogeneity resulting from mechanical stresses is more substantial. It was examined by light transmission in crossed polaroids (the stresses cause birefringence in BSO crystals). The crystal faceting is the main cause of this heterogeneity in BSO crystals. We have observed that it provides a characteristic distribution of the stresses due to anisotropy in the growth rate and impurity distribution coefficients. It is most pronounced in BSO:Cr crystals, while being weaker for undoped BSO crystals. We have established that the post-growth annealing in air at T_a = 770–970 K for 24 h followed by a slow temperature decrease down to room temperature during 10–15 h considerably relaxes both the radial and axial stresses the ones. In spite of the stresses resulting from faceting, the

Table 2. Influence of crystallization purification on the properties and homogeneity of BSO crystals

Physical characteristics	Charge	1st crystallization	2nd crystallization	3rd crystallization	4th crystallization
Uncontrolled impurity, p.c.mass., crystal/slag	$8.7\cdot10^{-2}$	$1.2\cdot10^{-2}$/ $9.5\cdot10^{-2}$	$4.5\cdot10^{-3}$/ $7.8\cdot10^{-3}$	$5\cdot10^{-3}$/ $6.5\cdot10^{-3}$	$5.7\cdot10^{-3}$/ $7\cdot10^{-3}$
Microscopic homogeneity	—	••	O	O	••
Light transmission in crossed polaroids, t, a.u.	—	15–20	7–10	10–15	20–25
PCE, $\Delta\alpha^{ph}$, cm^{-1} ($h\nu$ = 2.6–2.4 eV)	—	5–12	0–0.5	5–8	8–15
σ_i^{ph}, $\Omega^{-1}cm^{-1}$ ($h\nu$ = 2.6–2.4 eV)	—	$(2–3)\cdot10^{-10}$	$(2–3)\cdot10^{-10}$	$(2–5)\cdot10^{-10}$	$(2–5)\cdot10^{-10}$
α_0, cm^{-1} ($h\nu$ = 2.8–2.4 eV)	—	117–33.8	103.8–27	150–40	160–46

Notes: O, homogeneous crystal; ••, inclusions of about 10^{-3} cm in the crystal bulk.

face growth is preferable because it minimizes such heterogeneities as blocks, coarse inclusions, and dislocations. In general, the optimum conditions make it possible to grow by the Czochralski method the undoped BSO crystals of 40×40×120 mm^3 size which can be used as active optoelectronic media.

We have used the optimal growing conditions to grow doped BSO crystals, too. It has been shown [6] that a considerable number of sillenite phases of $Bi_{24}M^{3+}M^{5+}O_{40}$ and $Bi_{24}M^{2+}M^{6+}O_{40}$ type can be obtained using the M ion substitution. But the authors [6] have not investigated the possibility of the Bi^{3+} ions substitution by doping ions and the doping ion preference energy E_{pr} to the octahedral symmetry of the oxygen environment. The E_{pr} defines the of the total enthalpy variation with the change of the coordination polyhedron from tetrahedron to octahedron. The E_{pr} values were obtained by experimental calorimetry technique. It has also been shown that those are of importance for oxide crystals [7] and that E_{pr} should be taken into account when the localization of the doping ions in the lattice sites of doped spinels and in a number of laser crystals doped with transition metal ions.

The inclusion probability of the doping ions in BSO octa- and tetra-sites has been estimated taking into account E_{pr}. In the frame of isomorphism theory, the impurity distribution coefficient K_d for a low impurity concentration is described by the expression [8]:

$$\ln K_d \approx \approx R^{-1} \cdot [\Delta H_f(T_{cr}^{-1} - T_f^{-1}) - Q(1.2T_{cr}^{-1} - t^{-1})], \quad (4)$$

where ΔH_f is the melting heat; T_{cr}, the crystallization temperature; T_f, the melting temperature of the dopant; t = 1059 K, empirical constant, R = 8.314 J·(mol·K)$^{-1}$, the gas constant; Q, the mixing energy for the matrix/activator system [9]: $Q \approx Q_{1,2} = a(\Delta r/ R^*_{1,2})^2 + b(\Delta^i s)^2$, where a and b are constants; Δr, the ion radius difference for ions substituting one another, $R^*_{1,2}$ = 2.48 and 1.65 Å, the mean Bi–O and Si–O bond lengths, respectively; $\Delta^i s$, the difference of the ionicity degrees in the metal ion-oxygen ion system. The $^i s$ values have been estimated using the ratio [9]: $^i s \approx (\chi_N - \chi_0)/(\chi_N + \chi_0)$, where χ_N and χ_0 = 3.1 are the electro-negativity of the doping N-ion and oxygen ion O^{2-}, respectively. The influence of $\Delta r/R^*$ and $\Delta^i s$ on the $Q_{1,2}$ value is of a considerable interest. We have used the known for BSO K_d, ΔH_f, T_{cr}, T_f values and K_d = 0.2 (BSO:Al), 0.13 (BSO:Ga) [1] to estimate $a \approx 4.254\cdot10^6$, $b \approx 1.7\cdot10^7$ J·mol^{-1}, and then Q_1 and Q_2 energies corresponding to the cases of Bi^{3+} and Si^{4+} substitution by the impurity ions (Table 3). Taking into account of energy E_{pr}, the values of $Q^*_1 = Q_1 + E_{pr}$ and $Q^*_2 = Q_2 + E_{pr}$ have been o btained. The probability evaluation for the inclusion of impurity ions into the octa- and tetra-sites ($W_{Bi} \sim Q^{*}_1{}^{-1}$, $W_{Si} \sim Q^{*}_2{}^{-1}$, respectively) has shown that the crystal-chemical situation is energetically favorable for the inclusion of Cr^{3+}, Mn^{4+} and V^{2+} ions in octa-sites. Cr^{2+}, Mn^{3+}, Mn^{2+}, V^{3+}, V^{2+}, Fe^{2+}, Cu^{2+}, Cu^{+}, Ag^{3+}, Ag^{2+}, Ag^{+}, Sn^{4+}, Sn^{2+} ions

Table 3. Characteristics of impurity ion localization in BSO crystals

Ions	$Q_1 \cdot 10^{-3}$, J·mol^{-1}	$Q_2 \cdot 10^{-3}$, J·mol^{-1}	$E_{pr} \cdot 10^{-3}$, J·mol^{-1} [7]	K_d	K_d^{exp}; (crystal, K_d^{exp}, references)
Cr^{6+}	216	543	5.9	1.12	1.5;
Cr^{5+}	97	356	—	1.17	(BGO, 1.8; [1])
Cr^{4+}	75	275	—	1.19	—
Cr^{3+}	282	203	−137±10	2.1	—
Cr^{2+}	625	272	−29	0.84	—
Mn^{6+}	300	610	—	0.133	0.2
Mn^{5+}	151	416	—	0.139	—
Mn^{4+}	158	182	−43	0.146	—
Mn^{3+}	446	397	−50	0.14	—
Mn^{2+}	854	474	0±4	0.137	—
V^{5+}	1113	1627	−40.1	0.08	0.12
V^{4+}	165	271	−43.5	0.11	—
V^{3+}	434	402	−134	0.107	—
V^{2+}	657	337	—	0.109	—
Fe^{3+}	87	212	−22.2±3	0.17	0.07;
Fe^{2+}	211	164	—	0.172	(BGO, 0.05; [1])
Cu^{3+}	167	175	—	0.276	0.3
Cu^{2+}	371	62	−84	0.283	—
Cu^{+}	434	89	46	0.281	—
Ag^{3+}	395	57	—	1916.9	—
Ag^{2+}	756	16	—	18.6	—
Ag^{+}	1298	33	4.2	14.3	—
Mo^{6+}	180	343	—	0.778	1.1
Mo^{4+}	294	198	—	0.807	—
Mo^{3+}	375	216	—	0.803	—
Sn^{4+}	312	80	−59	0.34	0.5
Sn^{2+}	1518	67	—	0.342	—
Ga^{3+}	140	292	—	0.137	0.5; (BSO, 0.14;[1])
Al^{3+}	134	465	—	0.17	0.5; (BSO, BGO, 0.2; [1, 2])

Notes: parameters of ions: r = 1.16 Å, χ = 2 (Bi^{3+}) and r = 0.4 Å, χ = 1.9 (Si^{4+}); in brackets size K_d^{exp} on the data [1, 2]; BGO — crystals $Bi_{12}GeO_{20}$.

are more likely to be included in octa-sites than in tetra-sites, while Cr^{6+}, V^{5+}, Cr^{4+}, Al^{3+}, Ga^{3+}, Mn^{6+}, Mn^{5+}, Fe^{3+}, Mo^{6+} ions are preferred in tetra-sites (Table 3). These conclusions answer to the growing practice of sillenites. For example, Cr-, Mn- and V-sillenites with full substitution of Si by Cr, Mn or V ions are obtainable only in hard oxidizing conditions of hydrothermal synthesis, thus at an oxidation degree of Cr, Mn and V exceeding $^{3+}$, and the crystals are small in size (about 1 mm) [10]. Using Q_1^* and Q_2^* and expression (4), the impurity distribution coefficients K_d were calculated. As is seen, the experimentally evaluated coefficients K_d^{exp} correlate in most cases with the calculated coefficient K_d (Table 3).

Photochromic effect is considered to be an undesirable phenomenon as the BSO crystals are used in light-modulating de-

Table 4. PCE characteristics in undoped and doped BSO crystals

Crystal	$\Delta(h\nu)$, eV	$h\nu_{max}$, eV	Ξ, a.u.	K_r
BSO	2–3	1.5;2.3; 2.7	7.8	0.8
BSO:Al	0.5–1.5; 2–3.5	0.76;2.48	2.5	0.7
BSO:Ga	0.5–1.5; 2–3.5	0.8;2.35	3.1	0.6
BSO:Sn	0.5–1.5; 2–3.5	0.61;1.15;1.85; 2.1	3.5	0.7
BSO:Fe	2–3	2.71;2.84	4	0,8
BSO:Cu	0.5–1; 1.4–2	0.72;0.91;1.57;1.78	9	0.85
BSO:Cr	1.5–3	1.5;1.56;2.23;2.83	22	0.9
BSO:Mn	1.5–1.8; 2–3	1.51;1.59;2.19; 2.48	12	0.9
BSO:V	0.5–3.2	0.5;2.98	0.5	0.6
BSO:Ag	0.7–1.5; 2–3	0.9;1.15;1.3	5	0.8
BSO:Mo	1.7–3.2	2.2;2.65;2.8; 3.1	10	0.9

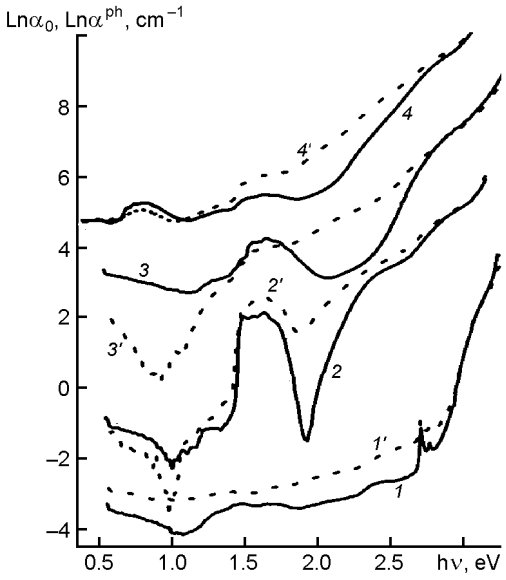

Fig. 1. Stationary (*1–4*) and photoinduced (*1′–4′*) absorption spectra in BSO:Fe (*1*, *1′*), BSO:Cr (a, *2*, *2′*), BSO:Mn (*3*, *3′*), BSO:Cu (*4*, *4′*) crystals. Curves are displaced vertically by 3 (*3*, *3′*), 6 (*4*, *4′*) and −3 (*1*, *1′*) log units. PCE is excited by light with quantum energy $h\nu$ = 2.85 eV during 120 s. T = 80 K.

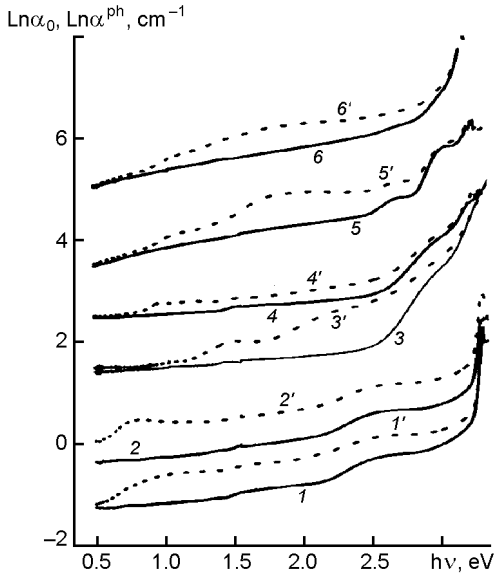

Fig. 2. Stationary (*1–6*) and photoinduced (*1′–6′*) absorption spectra in BSO:Ga (*1*, *1′*), BSO:Al (*2*, *2′*), BSO (*3*, *3′*), BSO:Ag (*4*, *4′*), BSO:Mo (*5*, *5′*), BSO:Sn (*6*, *6′*) crystals. Curves are displaced vertically by 0.5 (*2*, *2′*; *4*, *4′*), 2 (*5*, *5′*) and 5 (*6*, *6′*) log units. PCE is excited by light with quantum energy $h\nu$ = 2.85 eV during 120 s. T = 80 K.

vices working on the Pokkels effect. On the other hand, it is of importace in holographic information recording. Consequently, PCE is to be taken into account with different signs when estimating the optical quality of BSO crystals. The common concept of doping influence on PCE is provided by family of stationary and photoinduced absorption spectra (Figs.1, 2). Ions Cr, Mn, V, Fe, Cu, Ag, Mo exhibit the intercenter absorption bands, characteristic for their certain charge state. Further, we shall note that ions Al, Ga, Sn, and Fe weaken the stationary and photoinduced absorption over the whole spectrum (as compared to undoped BSO). Ions Cr, Mn, Cu amplify PCE considerably in the visible range while it falls in IR area. Ions Sn and Mo provide PCE in the visible spectral

range, comparable with that in BSO crystals, while ions Al, Ga, Sn, Ag give additional absorption bands in near IR range. In crystals BSO:V, PCE is weak in the whole spectrum. At room temperature, PCE decreases in the most part of crystals, but the general view of spectra does not change. However, in undoped BSO and BSO with Cr, Mn and Cu, PCE remains significant. The characteristics of practical importance: integrated PCE $\Xi = \int \Delta^{ph}\alpha(h\nu)d(h\nu)$, the reversibility coefficient K_r (the integrated PCE ratio in two successive "record-optical deleting" cycles), spectral range $\Delta(h\nu)$ and spectral positions of PCE band maxima $h\nu_{max}$ for the latter ion kinds at $T = 80$ K are presented in Table 4.

The results of investigation show that a further development of such photochromic materials as BSO crystals doped with Cu and Ag (the near IR range), Cr, Mn (red bands), Mo (dark blue and near UV-range) is of interest.

To conclude, technological growing possibilities of high-quality BSO crystal have been investigated. The optimum conditions have been determined for the quality improvement of undoped BSO crystals and BSO crystals doped with Al, Ga, Cr, Mn, V, Cu, Mo, Fe, Ag, and Sn grown by Czochralski method. The chare state and the localization of the dopant ions in BSO crystal lattice have been estimated in the frame of isomorphism theory taking into account the energy preference to octahedron oxygen environment. The distribution coefficients in BSO crystals have been determined for a number of doping ions. The PCE spectral characteristics for undoped and doped BSO crystals have been obtained.

References

1. B.C.Grabmaier, R.Obercshmid, *Phys. Stat. Sol(a)*, **96**, 199 (1986). V.K.Malinovsky, O.A.Gudaev, V.A.Gusev, S.I.Demenko, Photoinduced Phenomena in Sillenites, Nauka (Siberian Div.), Novosibirsk (1990) [in Russian].
2. H.Bou Rjeily, F.Ramaz, D.Petrova et al., *SPIE Proc.*, **3178**, 169 (1997).
3. T.V.Panchenko, Z.Z.Yanchuk, *Fiz. Tverd. Tela*, **38**, 3042 (1996).
4. J.C.Brice, T.M.Brutton, O.F.Hill, *J. Cryst. Growth*, **24/25**, 420 (1974).
5. Yu.F.Kargin, A.A.Mar'in, V.M.Skorikov, *Izv. AN SSSR:Neorg. Mater.*, **18**, 1605 (1982).
6. L.Ya.Raznitsky, *Izv. AN SSSR:Neorg. Mater.*, **20**, 1867 (1984).
7. V.S.Urusov, Theory of Isomorphic Mixibility, Nauka, Moscow (1977) [in Russian].
8. V.S.Urusov, Energy Crystal Chemistry, Nauka, Moscow (1975) [in Russian]. S.V.Fedotov, A.A.Bush, in: Abstr. of All-Union Conf. on Real Structure and Properties of Non-Centered Crystals, Part 1, VIEMS Publ., Moscow (1990), p.63 [in Russian].

Леговані кристали силеніту

Т.В.Панченко, Н.А.Трусєєва, К.Ю.Стрілець

Вирощено кристали $Bi_{12}SiO_{20}$ із варійованою концентрацією дефектів нестехіометрії та леговані іонами Al, Ga, Cr, Mn, V, Cu, Mo, Fe, Ag і Sn. У межах теорії ізоморфізму з урахуванням енергії переваги до октаедрічного кисневого оточення визначено локалізацію домішкових іонів у кристалічних гратках, знайдено коефіцієнти їх розподілу. Запропоновано методи підвищення оптичної якості чистих і легованих кристалів $Bi_{12}SiO_{20}$, досліджено їх фотохромні властивості.